

The Van der Laan extragalactic emission model applied to GRS 1915+105

Author: Milan Quandt Rodríguez

*Facultat de Física, Universitat de Barcelona, Diagonal 645, 08028 Barcelona, Spain.**

Advisor: Josep Maria Paredes Poy

Abstract: We apply the Van der Laan model to the microquasar GRS 1915+105 and extract parameters that fit the radio emission curves best. We obtain values for the energy spectral index in the range of $p \sim 0.7 - 0.8$ for the fit, which largely disagree with the ones predicted by the model, about $p \sim 0.1$. This results suggest that to model synchrotron radio emission of X-ray binaries we need to take into account events such as continuous injection and energy losses, as well as a jet-like geometry rather than a spherically symmetric one.

I. INTRODUCTION

Microquasars are binary stellar systems that can be understood as miniature replicates of quasars (Quasi Stellar Radio Sources), as they exhibit the three basic elements which characterize them; a black hole, an accretion disc and collimated jets of ultrarelativistic particles.

In a binary stellar system, in which an ordinary star is gravitationally linked to a black hole or neutron star and thus makes a closed orbital movement around it, the central compact object can suck matter from the star and create a so called accretion disc. In the case of a Black Hole, the characteristic timescale of the matter flowing onto it is proportional to it's mass, which allows us to study in minutes events that in quasars of $10^9 M_\odot$ could take up to thousands of years (Sams et al 1996; Rees 1998). Matter is heated in the accretion disc due to frictions between particles (viscous heating) to temperatures of order of 10^6 K and thus glows in X-ray (Mirabel & Rodríguez 1999).

Formation of high energy collimated jets is believed to be associated with the sudden disappearance of the inner accretion disc (X-ray dip). During this disappearance most of the material forming the disc is thought to be advected into the black hole, being only one part of it ejected as synchrotron-emitting clouds of plasma (Mirabel et al, 1998). A possible mechanism for the ejection of synchrotron radiating jets is given by the supercritical accretion mechanism. This phenomena occurs when during accretion the Eddington limit is overcome, this is, when $\dot{M}_{accr} > \dot{M}_{Edd}$. When this happens, material that was being accreted is violently rejected by the radiation pressure and a shock wave is produced which expands outwards from the central region. This event can provoke the ejection and acceleration of particles, and generate strong magnetic fields (Paredes et al, 1995). Of course there can be plenty of other possible mechanisms for accelerating electrons ejected in the accretion disc.

Clouds of relativistic particles ejected from the accretion disc are usually called plasmons.

As plasmons are ejected they are accelerated and can reach apparent superluminal velocities, due to relativistic aberration (Rees, 1966). The first superluminal galactic source discovered was GRS 1915+105 (Mirabel & Rodríguez, 1994) and allowed to study in detail all of the phenomena explained above.

II. THE VAN DER LAAN MODEL

The Van der Laan model (Van der Laan, 1966) was originally developed to explain the variability observed in quasars and describes the radio emission of spherically symmetric plasmons ejected from the accretion disc.

Suppose a uniform spherical cloud of radius r composed of a flux of relativistic electrons expanding at rate \dot{r} from an initial radius r_0 . The energy distribution of the relativistic electrons is taken to be $N(E)dE = K(t)E^{-p}dE$ ($E_1(t) \leq E \leq E_2(t)$), where N is the number density of the electrons, $K(t)$ a time-depending constant and p the energy spectral index.

As they are being accelerated in a magnetic field B , they will of course radiate. The model considers this field B to be uniform inside the spherical plasmon, and that its variation with time conserves magnetic flux, so that

$$B = B_0 \left(\frac{r}{r_0} \right)^{-2} \quad (1)$$

The relativistic gas is taken to cool adiabatically

$$E = E_0 \left(\frac{r}{r_0} \right)^{-1} \quad (2)$$

and variation of the instantaneous apparent size is just

$$\theta = \theta_0 \left(\frac{r}{r_0} \right) \quad (3)$$

where the subscript 0 denotes the values of the parameters at a specific instant t_0 and the ratio $\frac{r}{r_0}$ is usually denoted as ρ , the relative radius of the plasmon.

*Electronic address: milanq@gmail.com

Another important feature of the Van der Laan model is that, there's no variation in the number of particles forming the plasmon, this is:

$$\frac{d}{dt} \left[r^2(t) K(t) \int_{E_1}^{E_2} E^{-p} dE \right] = 0 \quad (4)$$

In the synchrotron radiation process the absorption and emission coefficients depend on the frequency, respectively, like; $\mu(\nu)\nu^{-(p+4)/4}$ and $p(\nu) \propto \nu^{-(p-1)/2}$ and thus, we can express the frequency dependance of the spectral curve like:

$$S(\nu) \propto \frac{p(\nu)}{\mu(\nu)} [1 - e^{-\tau(\nu)}] \propto \nu^{5/2} [1 - e^{-\tau(\nu)}] \quad (5)$$

where $\tau(\nu) \propto \nu^{-(p+4)/2}$.

Solving

$$\frac{dS(\nu)}{d\nu} = 0 \quad (6)$$

gives the condition for the optical depth to be maximum:

$$e^{\tau_m} - \frac{p+4}{5} \tau_m - 1 = 0 \quad (7)$$

Note that the model assumes that initially, the plasmon is compact enough to be optically thick at all radio frequencies, and it will become optically thin at some point during its expansion. From (5) we see that in the optically thick region ($\nu \ll 1$) the spectral curve is given by the source function $\frac{p(\nu)}{\mu(\nu)}$ and thus has the form $S(\nu) \propto \nu^{5/2}$. On the other hand, when the cloud becomes optically thin ($\nu \gg 1$), we have that $S(\nu) \propto \nu^{-\frac{1-p}{2}}$.

Van der Laan also obtained the radius dependance of frequency and flux density which go like:

$$\nu_m(\rho) = \nu_{m0} \rho^{-(4p+6)/(p+4)} \quad (8)$$

$$S_m(\rho) = S_{m0} \rho^{-(7p+3)/(p+4)} \quad (9)$$

The model thus predicts that when observing the source at a given frequency, it will show a rapid increase in flux at first, peak at a maximum S_m and decrease more gently. Observations at lower frequencies will show curves with same proportion but will peak later and will have a smaller value.

The flux density at any given frequency and radius relative to their values at t_0 by the Van der Laan model is then expressed as:

$$S(\nu, \rho) = S_{m0} \left(\frac{\nu}{\nu_{m0}} \right)^{\frac{5}{2}} \rho^3 \frac{[1 - \exp(-\tau_m \left(\frac{\nu}{\nu_{m0}} \right)^{-\frac{(p+4)}{2}} \rho^{-(2p+3)})]}{1 - \exp(-\tau_m)} \quad (10)$$

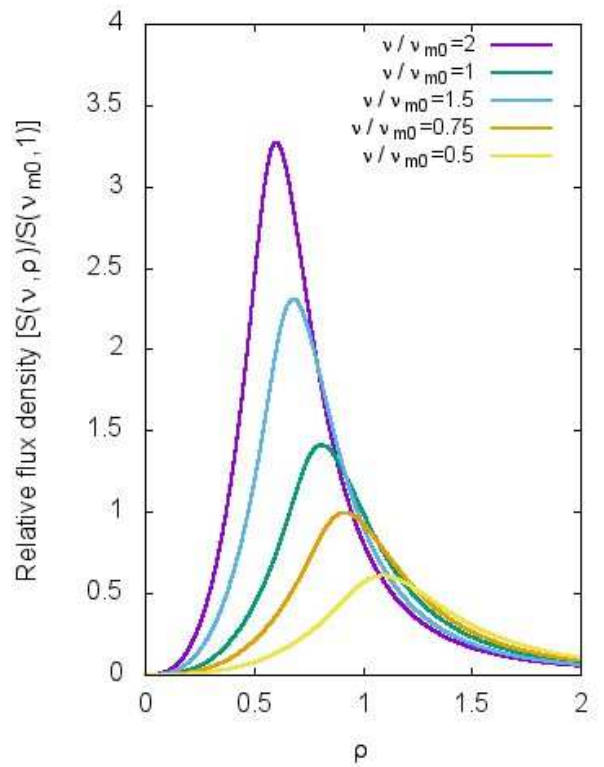


FIG. 1: Evolution of the flux density with increasing radius. All curves have been plotted with a value of energy spectral index $p = 2$

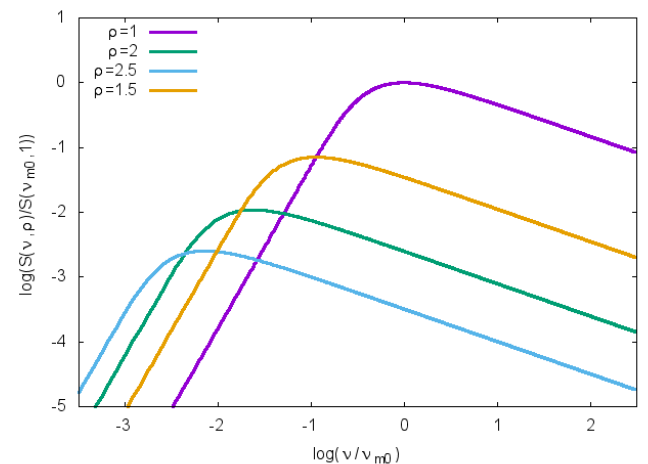


FIG. 2: Evolution of the flux density with frequency. All curves have been plotted with a value of energy spectral index $p = 2$

Figure 1 shows the evolution of the flux density with increasing radius for different frequencies, and figure 2 the time evolution of the spectrum with different values of the relative radius ρ .

Note that expression (10) does not give us the time-dependance of the flux density. If we assume that the

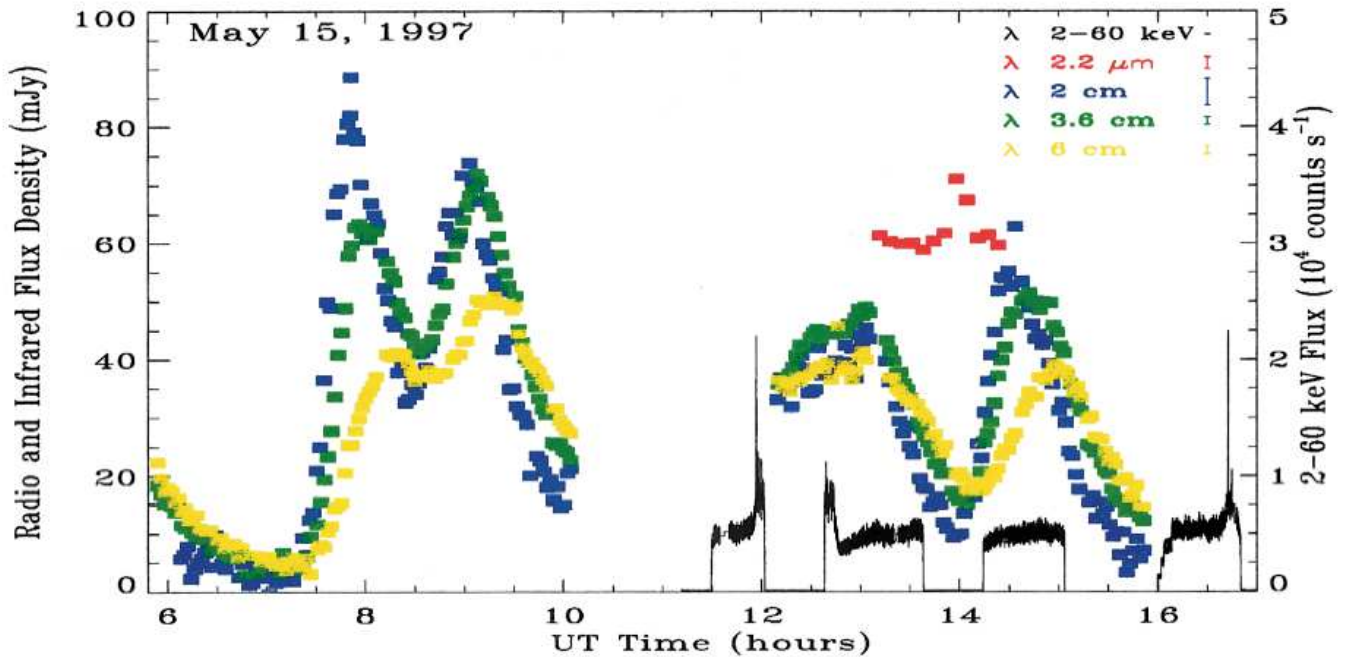


FIG. 3: Radio, infrared and X-ray curves of GRS 1915+105 (Mirabel et al, 1998). Data corresponds to observations done on May 15, 1997 with the VLA at 2, 3.6 and 6 cm, with UKIRT at $2.2\mu\text{m}$, and the PCA of RXTE at 2-60 keV. Units on the left side for y axis correspond to infrared and radio curves, while those on the right correspond to X-ray observation. Representative error bars of the different wavelengths are also shown.

plasmon expands with constant velocity, radius will vary like $r = r_0 + vt$ and thus we can write:

$$\rho(t) = \frac{r}{r_0} = 1 + \frac{vt}{r_0} = 1 + \frac{t'}{t_0} \quad (11)$$

where the observed expanding velocity v of GRS1915+105 is approximately $\sim 0.2c$ (Mirabel et al 1998) and t' is the time measured from the instant where S_0 and ν_{m0} are specified.

In the model, the variation of the maximum flux density goes like:

$$S_{m,\lambda} \propto \lambda^{-(7p+3)/(4p+6)} \quad (12)$$

and is reached at:

$$t_{m,\lambda} \propto \lambda^{-(p+4)/(4p+6)} \quad (13)$$

These two last equations will then permit us to calculate spectral changes in the immediate future (for later times they depend on the expansion mode).

III. GRS 1915+105

GRS 1915+105 is a galactic X-ray binary which was discovered in 1992 by the WATCH all-sky monitor on board the soviet GRANAT satellite (Castro-Tirado A. J.

et al 1992), but didn't become famous until radio observations showed superluminal motions of its jets, making it the first ever superluminal galactic source observed (Mirabel & Rodríguez, 1994). It lies at about 11 kpc away in Aquila constellation (Fender et al, 1999) and although its optical counterpart is unknown due to large extinction, its radio, infrared and X-ray observations have suggested analogies with the much bigger extragalactic quasars and has therefore provided a perfect laboratory to understand events that take place in this much larger objects, such as how particles are ejected and accelerated in the accretion disc instabilities (Türler, 2004).

Data we use here are the radio oscillation events of GRS 1915+105 reported on May and September 1997 with the 27 antennae of the Very Large Array (VLA) in the three radio wavelengths of 2, 3.6 and 6 cm (Mirabel et al, 1998), as can be seen in figure 3.

IV. RESULTS AND DISCUSSION

In order to apply the model to the data we will perform a least squares fit and obtain the parameters that fit the curve best.

We will study the particular case of the last flare observed in figure 3, between $\sim 14\text{h}$ and 16h (UT time), as it appears more isolated.

First of all, we note that the time lapse between two successive outbursts is small enough to overlap the tail

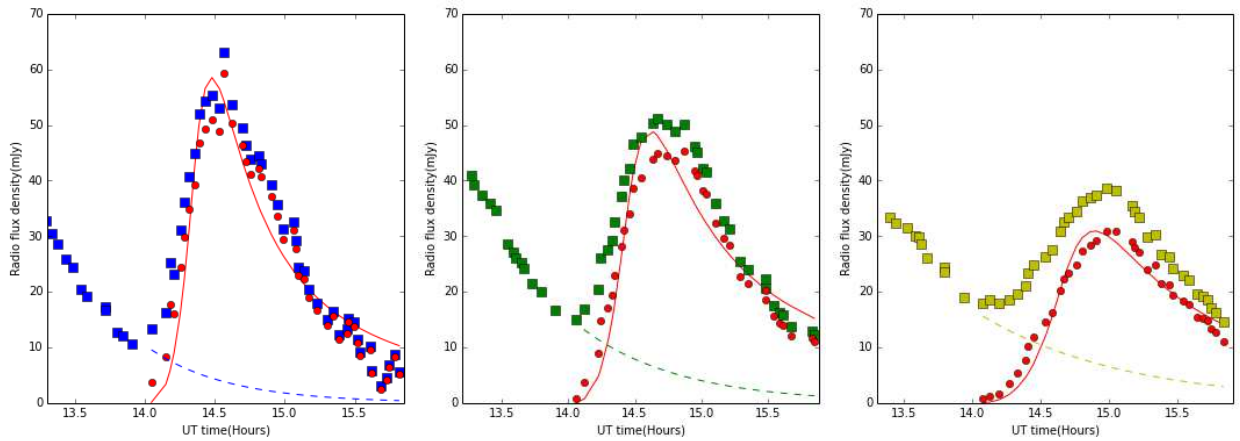


FIG. 4: Corrections for all three different wavelengths of 2, 3.2 and 6 cm respectively. Note that we plot data obtained with VLA with the same colors as in figure 3. Red points correspond to contamination free data and red line is the fit to the model. Dashed lines represent the interpolated contribution of the decaying jet.

of one preceding burst with the rise of the following one. This is known as *contamination* and our first step in order to obtain successful results will be to eliminate it. To do this, we interpolate the missing points of the preceding jet's tail (the curve between ~ 12 h and 14h) and just subtract its contribution to ours. Note that the 6cm curve is the most contaminated, because the preceding flare in this same wavelength λ will extend wider in the region of our last flare.

Once applying this correction to the data, we obtain these different values for the three different wavelengths:

| λ (cm) | ν (GHz) | $S_{m,\lambda}$ (mJy) |
|----------------|-------------|-----------------------|
| 2 | 15 | 59.32 |
| 3.6 | 8.33 | 45.35 |
| 6 | 5 | 30.98 |

TABLE I: Wavelength, frequency and peak flux density corresponding to data of the last flare

After removing *contamination*, we proceed to fit our curves using the least squares method. Figure 4 shows the corrections applied to the data and their corresponding fit. We permit all five parameters that appear in the Van der Laan model to change freely in order to obtain values for them which fit the data best.

We determine that values of the energy spectral index p for each of the different wavelengths are:

| λ (cm) | p |
|----------------|------|
| 2 | 0.78 |
| 3.6 | 0.68 |
| 6 | 0.79 |

TABLE II: Values of the energy spectral index that fit best each of the different wavelengths

This tells us that that the expected value of p should be in the range of ~ 0.7 to 0.8 .

To test this result, we can perform a calculation based on the relation between flux density and wavelength of equation (12) and obtain the value of p predicted by the model. Then, taking values for $S_{m,\lambda}$ for $\lambda = 2$ cm and $\lambda = 3.2$ cm from table 1 we have that:

$$\frac{59.32 \text{ mJy}}{45.39 \text{ mJy}} = \frac{(2 \text{ cm})^{-\frac{(7p+3)}{(4p+6)}}}{(3.2 \text{ cm})^{-\frac{(7p+3)}{(4p+6)}}} \Rightarrow p \simeq 0.12 \quad (14)$$

and we get a very similar result by taking for example $\lambda = 2$ cm and $\lambda = 6$ cm:

$$\frac{59.32 \text{ mJy}}{30.98 \text{ mJy}} = \frac{(2 \text{ cm})^{-\frac{(7p+3)}{(4p+6)}}}{(6 \text{ cm})^{-\frac{(7p+3)}{(4p+6)}}} \Rightarrow p \simeq 0.12 \quad (15)$$

Thus, we can clearly see that values for p predicted by the model largely disagree with those that fit the curves best. This inconsistency evidences the inability of the Van der Laan model to correctly describe synchrotron emission of this source.

V. CONCLUSIONS

This work shows that the Van der Laan model fails when modeling different synchrotron radio emission curves of a X-ray binary like, in this case, the ones of GRS 1915+105. This suggests that there are different features in this kind of systems that aren't taken into account by the model; on the one hand, the model takes the plasmons ejected from the accretion disc to be spherically symmetric. Observations of this kind of systems show always jet-like geometry, and thus a more realistic geometry of the ejected plasmons could provide an improve in the model. On the other hand, equation (4) states

that the number of particles inside the expanding bubbles stays always constant, and does therefore not take into account neither continuous injection of relativistic electrons produced by acceleration mechanisms, neither the energy losses of this particles by different processes. In order to be able to predict correct values for X-ray binary radio emission, we should implement all of this phenomena in our model.

Acknowledgments

I want to express my gratitude to my advisor Dr. Josep Maria Paredes Poy for his patient and always very clear and helpful guidance through the development of this work. I also thank my family, who always helped me and provided financial support throughout the years.

-
- [1] Castro-Tirado A. J., Brandt S., Lund N., 1992, IAUC, 5590, 2
 - [2] Fender R.P., Garrington S.T., McKay D.J. et al, 1999, Monthly Notices of the Royal Astronomical Society, 304, 4
 - [3] Mirabel I.F., Rodríguez L.F., 1994, Nat, 371:46-48
 - [4] Mirabel I.F., Dhawan V., Chaty S., Rodríguez L.F., Martí J., Robinson C.R., Swank J., Geballe T.R., 1998, A&A, 330, L9
 - [5] Mirabel I.F., Rodríguez L.F., 1999, A&A phys. rev., 37:40943
 - [6] Paredes J.M., Martí J., Estalella R., Peracaula M., 1995, Revista de física, 9, 17-24
 - [7] Rees M.J., 1966, Nature, 211:468-70
 - [8] Rees M.J., 1998, University of Chicago press, pp. 79-101
 - [9] Sams B.J., Eckart A., Sunyaev R., 1996, Nature, 382:47-49
 - [10] Türler M., Courvoisier T.J.-L., Chaty S., Fuchs Y., 2004, A&A 415:35-38
 - [11] van der Laan H., 1966, Nature, 211:1131-33